Altered hemodynamics during arteriovenous fistula remodeling leads to reduced fistula patency in female mice

Tambudzai Kudze, MD, MHS,[a] Shun Ono, MD,[b] Arash Fereydooni, MS,[a] Luis Gonzalez, BS,[a] Toshihiko Isaji, MD, PhD,[a] Haidi Hu, MD, PhD,[a] Bogdan Yatsula, PhD,[a] Ryosuke Taniguchi, MD, PhD,[a] Jun Koizumi, MD, PhD,[b] Toshiya Nishibe, MD, PhD,[c] *and* Alan Dardik, MD, PhD,[a,d,e] *New Haven and West Haven, Conn; and Isehara and Tokyo, Japan*

ABSTRACT

Objective: The arteriovenous fistula (AVF) is the preferred method of dialysis access because of its proven superior long-term outcomes. However, women have lower rates of AVF patency and utilization than men. We used a novel mouse AVF model that recapitulates human AVF maturation to determine whether there are differences in AVF patency in female and male mice.

Methods: Aortocaval fistulas were created in female and male C57BL/6 mice (9-10 weeks). At days 0, 3, 7, and 21, infrarenal inferior vena cava (IVC) and aortic diameters and flow velocity were monitored by Doppler ultrasound and used to calculate the vessel diameter, blood flow, and shear stress. AVF were harvested, and expression of proteins was examined by proteomic analysis and immunofluorescence and of messenger RNA by quantitative polymerase chain reaction analysis.

Results: At baseline, female mice weighed less and had lower IVC velocity and smaller magnitudes of shear stress, but there was no significant difference in IVC diameter and thickness. After AVF creation, both female and male mice had similar IVC dilation and thickening with no significant differences in IVC wall thickness at day 21. However, female mice had diminished AVF patency by day 42 (25.7% vs 64.3%; $P = .039$). During fistula remodeling, female mice had lower IVC mean velocity and shear stress magnitude and increased spectral broadening (days 0-21). Messenger RNA and protein expression of Krüppel-like factor 2, endothelial nitric oxide synthase, and vascular cell adhesion molecule 1 was similar at baseline in female and male mice but increased in the AVF only in male mice but not in female mice (day 21). Proteomic analysis of female and male mice detected 56 proteins expressed at significantly higher levels in the IVC of female mice and 67 proteins expressed at significantly higher levels in the IVC of male mice (day 7); function-specific analysis showed that the IVC of male mice overexpressed proteins that belong to pathways implicated in the regulation of vascular function, thrombosis, response to flow, and vascular remodeling.

Conclusions: AVF in female mice have diminished patency, preceded by lower velocity, reduced magnitudes of shear stress, and less laminar flow during remodeling. There is also sex-specific differential expression of proteins involved in thrombosis, response to laminar flow, inflammation, and proliferation. These findings suggest that hemodynamic changes during fistula maturation may play an important role underlying the diminished rates of AVF utilization in women. (JVS—Vascular Science 2020;1:42-56.)

Clinical Relevance: Women have lower rates of arteriovenous fistula (AVF) utilization than men. Using a mouse AVF model that recapitulates human AVF maturation, we show that female mice have similar AVF remodeling but diminished patency. AVF remodeling in female mice is associated with reduced shear stress and laminar flow; lack of increased transcription and translation of several anti-inflammatory, antiproliferative, and laminar flow response proteins (endothelial nitric oxide synthase, Krüppel-like factor 2, and vascular cell adhesion molecule 1); and different patterns of expression of pathways that regulate thrombosis and venous remodeling. Identifying downstream targets involved in these mechanisms may improve AVF outcomes in female patients.

Keywords: Arteriovenous fistula; Patency; Female sex; Laminar flow; Shear stress

From the Vascular Biology and Therapeutics Program,[a] and Division of Vascular and Endovascular Surgery, Department of Surgery,[d] Yale School of Medicine, New Haven; the Department of Diagnostic Radiology, Tokai University School of Medicine, Isehara[b]; the Department of Cardiovascular Surgery, Tokyo Medical University, Tokyo[c]; and the Department of Surgery, VA Connecticut Healthcare Systems, West Haven.[e]

This work was supported by U.S. National Institutes of Health grants R01-HL128406 and R01-HL144476 (to A.D.), Howard Hughes Medical Institute Medical Research Fellowships (to T.K. and A.F.), Society for Vascular Surgery Research Fellowship (to A.F.), and American Heart Association Fellowship (to A.F.) as well as with the resources and the use of facilities at the VA Connecticut Healthcare System (West Haven, Conn). The funding agencies had no involvement in any aspect of the creation of this manuscript.

Author conflict of interest: none.

Presented at the Vascular Research Initiatives Conference, San Francisco, Calif, May 9, 2018.

Correspondence: Alan Dardik, MD, PhD, Vascular Biology and Therapeutics Program, Yale School of Medicine, 10 Amistad St, Rm 437, PO Box 208089, New Haven, CT 06520-8089 (e-mail: alan.dardik@yale.edu).

The editors and reviewers of this article have no relevant financial relationships to disclose per the JVS-Vascular Science policy that requires reviewers to decline review of any manuscript for which they may have a conflict of interest.

2666-3503

https://doi.org/10.1016/j.jvssci.2020.03.001

Arteriovenous fistulas (AVF) are the preferred conduit for vascular access.[1,2] Before initiation of hemodialysis, AVF must mature, that is, thicken, dilate, and increase flow. However, AVF may fail to mature before clinical use (early failure) because of lack of venous remodeling, or they may fail after clinical use (late failure) because of development of neointimal hyperplasia.[3,4] Among risk factors associated with AVF failure, female sex is one of the top predictors.[5-7] Multiple clinical studies have reported that AVF in female patients have prolonged maturation time, decreased patency, and increased early thrombosis, preventing optimal AVF use.[8-10] Miller et al[9] reported reduced fistula adequacy for dialysis in women compared with men (31% vs 51%) in both upper and forearm fistulas and that women needed more salvage procedures than men (42% vs 23%).

No studies have yet identified the underlying mechanisms and pathophysiologic processes of the lower AVF maturation rates in women. Some of the speculated risk factors for AVF failure in women are smaller vessel diameter[11,12] and sex differences in vascular reactivity and platelet aggregation after vascular injury.[9] However, none of these factors has been conclusively identified as the mechanism of worse clinical performance.[13] We have previously used a mouse aortocaval fistula model that recapitulates human AVF maturation to study molecular mechanisms involved in venous remodeling.[14,15] This model shows wall thickening and diameter expansion between days 0 and 28, mimicking human AVF maturation, as well as increased neointimal hyperplasia and loss of patency in approximately one-third of male C57BL/6 mice between days 28 and 42, mimicking human AVF failure.[14,15] However, these previously reported studies were performed only in male C57BL/6 mice. Therefore, we used this model in both female and male age-matched mice to test the hypothesis that female mice have worse AVF patency compared with male mice because of the sex-specific differences in hemodynamics.

ARTICLE HIGHLIGHTS

- **Type of Research:** Basic science research
- **Key Findings:** Arteriovenous fistulas in female mice have diminished patency, lower velocity, reduced magnitudes of shear stress, and less laminar flow during fistula remodeling. There is sex-specific differential expression of proteins involved in thrombosis, response to laminar flow, inflammation, and proliferation.
- **Take Home Message:** Sex-specific differences in hemodynamic changes and the differential expression pattern of proteins that regulate response to laminar flow as well as thrombosis and venous remodeling during fistula remodeling may play a role in the diminished rates of arteriovenous fistula patency and utilization in women.

METHODS

AVF creation. All animal experiments were performed in strict compliance with federal guidelines and with approval from the Institutional Animal Care and Use Committee of Yale University. Female and male C57BL/6 mice aged 9 to 11 weeks were used in all experiments. Using 4% isoflurane in 0.8 L/min oxygen for induction and then 2% to 3%, mice were anesthetized for procedures. A midline laparotomy was performed under anesthesia, after which the aorta and inferior vena cava (IVC) were exposed. In a similar manner, the distal aorta was dissected for needle puncture, but the IVC was not dissected away from the aorta. After clamping just below the left renal artery, a 25-gauge needle was used to puncture the aorta into the IVC. For hemostatic compression, the surrounding tissue was used. Of note, the operators were not blinded to the sex of the mice. Visible pulsatile arterial blood flow in the IVC and hemostasis were used as markers of successful AVF creation.[14]

Ultrasound. Doppler ultrasound was used to measure preoperative and postoperative venous and arterial diameter and velocities in longitudinal view. Using 4% isoflurane in 0.8 L/min oxygen for induction and then 2% to 3%, C57BL/6 mice were anesthetized for procedures. The Vevo 770 High Resolution Imaging System (VisualSonics, Toronto, Ontario, Canada) with probe RMV704 (20-0 MHz) was used in all experiments. To confirm presence of the AVF, the waveforms in the IVC and aorta were recorded using the pulse wave mode in longitudinal view. In patent AVF, presence of the arterial or turbulent waveforms in the IVC and increased end-diastolic velocity in the aorta were used as markers of patency. Diameters of the aorta and IVC just above and caudal to the left renal vein were measured. Relative diameter was defined as the ratio of the vessel diameter at the specified time of measurement to the diameter measured at baseline (day 0). Ultrasound measurements were collected from the infrarenal aorta or the IVC and cranial to the site of AVF creation (Supplementary Fig, *A*) on preoperative day 0 and on postoperative days 3, 7, 14, and 21.

Using the IVC and aortic diameters and velocities, shear stress was then calculated by the following Hagen-Poiseuille formula:

$$T = 4\eta V/r$$

where T is shear stress, η is blood viscosity, V is flow velocity (in centimeters per second), and r is the radius (in centimeters). Blood viscosity was assumed to be constant at 0.035 poise. Spectral broadening was calculated using

the formula peak systolic velocity – width of spectral window.

Histology and wall thickness. The infrarenal (2 mm below from left renal vein) aorta and IVC were harvested at days 0, 7, and 21. The circulatory system was flushed under pressure with phosphate-buffered saline (PBS) followed by 10% formalin, and the AVF was extracted en bloc. The tissue block was embedded in paraffin and cut into 5-μm cross sections and stained with elastin-van Gieson. Intima-media venous wall thickness was measured using ImageJ software (National Institutes of Health, Bethesda, Md). Wall thickness was measured at four equidistant points per cross section and averaged.

RNA extraction and quantitative polymerase chain reaction (PCR). The arterial and venous limbs of the AVF were dissected and separated; care was taken to avoid surrounding tissue. Total RNA was isolated using the RNeasy Mini Kit with digested DNase I (Qiagen, Valencia, Calif). RNA quality was confirmed by the 260/280-nm ratio. Using the SuperScript III First-Strand Synthesis SuperMix (Invitrogen, Carlsbad, Calif), real-time quantitative PCR was performed using SYBR Green Supermix (Bio-Rad Laboratories, Hercules, Calif) and amplified for 40 cycles using iQ5 Real-Time PCR Detection System (Bio-Rad Laboratories). Correct target amplification was confirmed by 1.5% agarose gel electrophoresis, and primer efficiencies were determined by melt-curve analysis. We used glyceraldehyde-3-phosphate dehydrogenase RNA amplification for all sample normalization. Primers were provided by the Keck Oligonucleotide Synthesis facility at Yale University (Supplementary Table I).

Immunofluorescence. Tissue sections were deparaffined using xylene and a graded series of alcohols. Sections were heated in citric acid buffer (pH 6.0) at 100°C for 10 minutes for antigen retrieval. The sections were blocked with 5% bovine serum albumin in PBS containing 0.05% Triton X-100 (T-PBS) for 1 hour at room temperature before incubation overnight at 4°C with the primary antibodies diluted in T-PBS. Primary antibodies are listed in Supplementary Table II. Sections were then treated with secondary antibodies at room temperature for 1 hour using goat anti-rabbit Alexa Fluor 488 (Life Technologies), donkey anti-goat Alexa Fluor 488 (Life Technologies), or donkey anti-rabbit Alexa Fluor 568 (Life Technologies). Sections were stained with SlowFade Gold Antifade Mount with DAPI (Life Technologies), and a coverslip was applied. Digital fluorescence images were captured, and intensity of immunoreactive signal was measured using ImageJ software. Intensity of the merge signal was determined by applying a color threshold selective for the appropriate signal.

Proteomics and criteria for protein identification. To determine the steady-state protein levels in AVF from both sexes, we estimated protein composition of the AVF by mass spectrometry (MS)-based proteomics and label-free quantification analysis. The differences of protein abundance were analyzed by comparing the normalized intensity on distinct proteins from three or four different samples per group. Quantification was performed in a label-free format with the MaxQuant algorithms, using the normalized intensity values (label-free quantification intensity). Only proteins that were quantified in at least three experiments in one condition were included. Scaffold (version Scaffold_4.9.0; Proteome Software Inc, Portland, Ore) was used to validate MS/MS-based peptide and protein identifications. Peptide identifications were accepted if they could be established at >95.0% probability by the Scaffold Local FDR algorithm. Protein identifications were accepted if they could be established at >99.0% probability and contained at least two identified peptides. Protein probabilities were assigned by the ProteinProphet algorithm.[16] Proteins that contained similar peptides and could not be differentiated on the basis of MS/MS analysis alone were grouped to satisfy the principles of parsimony. Proteins sharing significant peptide evidence were grouped into clusters. Proteins were annotated with Gene Ontology terms from the National Center for Biotechnology Information (downloaded August 19, 2019).[17]

Experimental design. The wall thickness of the IVC was measured at baseline (day 0) immediately before AVF creation. During the early remodeling phase (days 0-21), the weight of the C57BL/6 mice as well as the hemodynamic parameters of interest (diameter, velocity, flow, and shear stress) were measured in the aorta and the IVC. Proteomic translational data were collected during the early remodeling phase (day 7). Immunofluorescence and quantitative PCR were performed at baseline (day 0) and at the end of the early remodeling phase (day 21). AVF patency was assessed up to day 42 (Supplementary Fig, *C*).

Statistical analysis. All data were analyzed using Prism 7 software (GraphPad Software, Inc, La Jolla, Calif). Kaplan-Meier curves were constructed for AVF patency rate analysis.

RESULTS

Female mice have reduced venous shear stress at baseline. To study differences in venous remodeling between female and male C57BL/6 mice, we used a mouse AVF model that recapitulates human AVF maturation.[15] Mice aged 9 to 10 weeks were weighed at baseline before surgery (day 0); female mice weighed less than similarly aged male mice (Fig 1, *A*). Before surgery, there was no difference in wall thickness in the IVC between

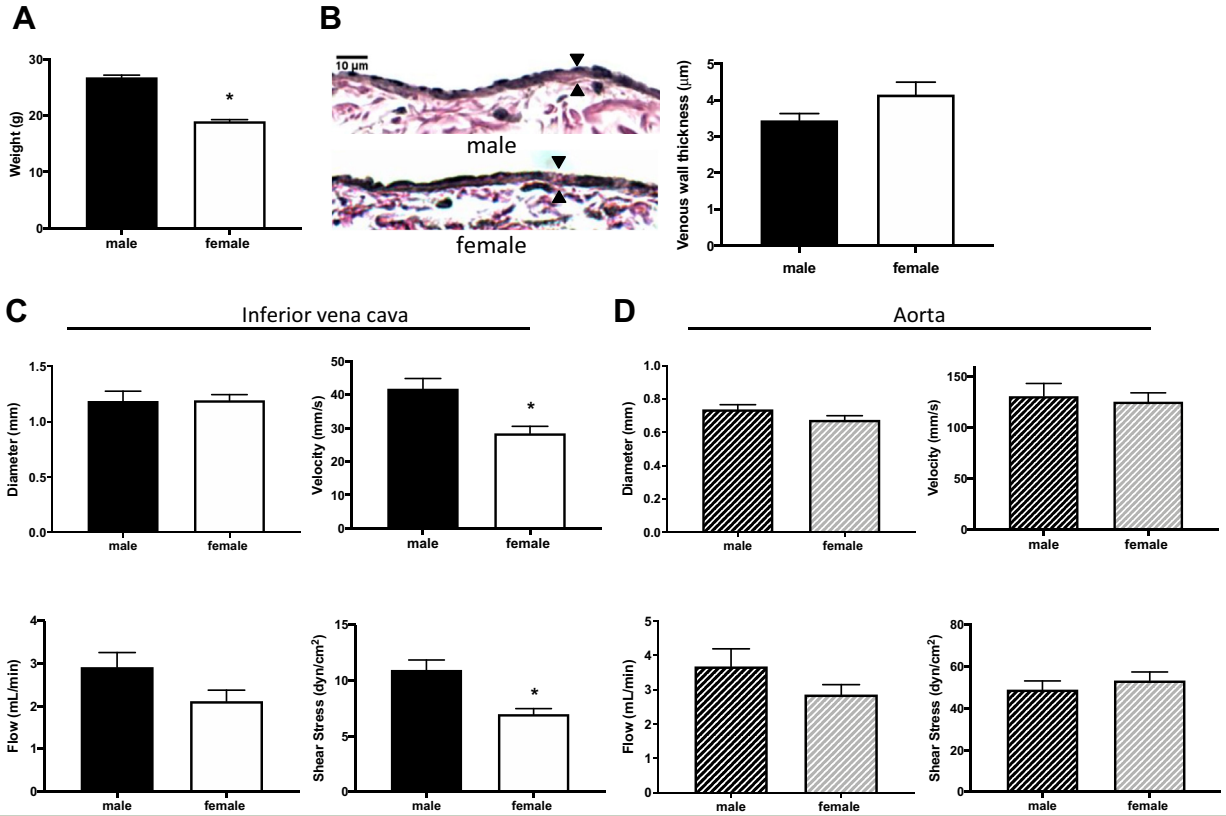

Fig 1. Female mice have reduced venous shear stress at baseline. **A,** Bar graph showing weight of male vs female mice at day 0: 26.85 ± 2.14 g vs 19.04 ± 1.43 g ($P < .0001$, *t*-test; n = 24-27). **B,** *Left*, Representative photomicrographs showing arteriovenous fistula (AVF) wall thickness in male vs female mice (day 0); *scale bar*, 10 μm. *Right*, Bar graph showing AVF wall thickness in male vs female mice: 3.20 ± 0.44 μm vs 4.15 ± 0.7 μm ($P = .9128$, *t*-test; n = 7-8). **C,** Bar graphs showing comparison in male vs female mice at day 0 (n = 14-22) of infrarenal inferior vena cava (IVC) diameter: 1.188 ± 0.3077 mm vs 1.194 ± 0.1857 mm ($P = .9503$, *t*-test); velocity: 41.87 ± 13.18 mm/s vs 28.5 ± 10.3 mm/s (*$P = .0002$, *t*-test); flow: 2.911 ± 1.417 mL/min vs 2.117 ± 1.201 mL/min ($P = .0661$, *t*-test); and shear stress: 10.94 ± 3.715 dyn/cm^2 vs 6.971 ± 2.284 dyn/cm^2 (*$P = .0003$, *t*-test). **D,** Bar graphs showing comparison in male vs female mice at day 0 (n = 14-25) of infrarenal aorta diameter: 0.738 ± 0.1272 vs 0.6757 ± 0.1144 ($P = .0983$, *t*-test); velocity: 130.6 ± 52.49 mm/s vs 125.1 ± 42.8 mm/s ($P = .7102$, *t*-test); flow: 3.679 ± 2.168 mL/min vs 2.856 ± 1.384 mL/min ($P = .1472$, *t*-test); and shear stress: 48.99 ± 17.64 dyn/cm^2 vs 53.35 ± 19.74 dyn/cm^2 ($P = .3973$, *t*-test).

female mice and male mice (Fig 1, *B*), and there was no difference in IVC diameter (Fig 1, *C*). In female mice, there was a trend toward less laminar flow in the IVC, with reduced mean velocity as well as mean magnitude of shear stress (Fig 1, *C*). However, there was no difference in diameter, velocity, flow, or mean shear stress magnitude in the aorta of female and male mice (Fig 1, *D*). Simple linear regression showed no significant relationship between weight and flow rate in the IVC (female, $P = .6749$; male, $P = .443$) or the aorta (female, $P = .1162$; male, $P = .8012$) of mice. There were similar amounts of spectral broadening in the IVC between female mice and male mice (37.37 ± 12.2 mm/s vs 29.74 ± 16.1 mm/s; $P = .9249$).

Female mice have similar AVF maturation but reduced patency. The C57BL/6 mouse aortocaval fistula model recapitulates human AVF maturation because there is wall thickening and dilation between days 0 and 28, similar to the thickening and dilation that occur during human AVF maturation.[15] AVF were created in both female and male mice (day 0).[14,15] There was no difference in the technical success rate of AVF creation in female mice compared with male mice (83% vs 88%; $P = .8132$, χ^2 test; Supplementary Fig). After AVF creation, weight gain was similar between female mice and male mice, although female mice continued to weigh less than male mice (Fig 2, *A*). Female and male mice had similar relative IVC (Fig 2, *B*) and aorta (Fig 2, *C*) diameters postoperatively; there was also no significant difference in the amount of wall thickening between female mice and male mice at day 21 (Fig 2, *D* and *E*). These data show similar AVF remodeling in female and male mice in this model.

In the mouse model between days 28 and 42, there is perianastomotic neointimal hyperplasia and consequent loss of patency in approximately one-third of male mice,

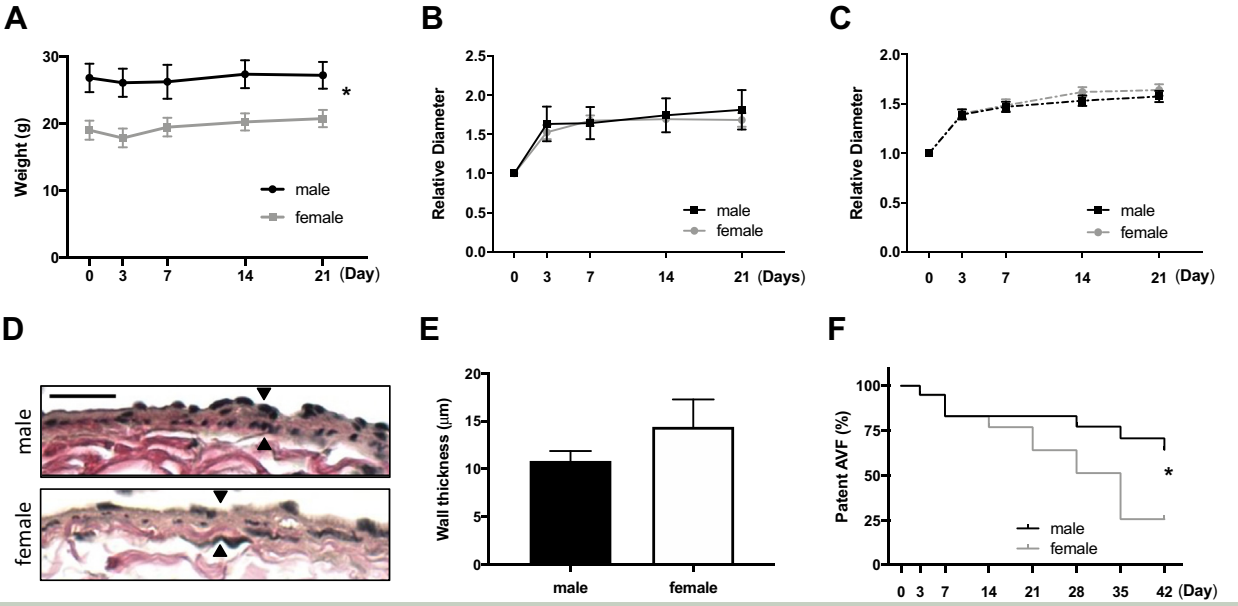

Fig 2. Female mice have similar early arteriovenous fistula (*AVF*) remodeling but reduced patency. **A,** Weight of mice at preoperative day 0 and postoperative days 3, 7, 14, and 21 ($P < .0001$, analysis of variance [ANOVA]). **B,** Line graphs showing relative diameter of inferior vena cava (IVC; $P < .0001$, ANOVA). **C,** Line graphs showing relative diameter of aorta ($P < .0001$, ANOVA). **D,** Representative photomicrographs showing AVF wall thickness in male vs female mice (day 21); *scale bar*, 25 μm. **E,** Bar graph showing AVF wall thickness in male vs female mice: 10.85 ± 3.244 μm vs 14.40 ± 9.937 μm ($P = .2931$, *t*-test; n = 10-12). **F,** Line graph showing AVF patency rate in male vs female mice up to day 42 (*$P = .0392$, log-rank; n = 19-20 in each group).

recapitulating the late functional outcomes of human AVF.[15] However, female mice showed reduced AVF patency by day 42 (25.7% vs 64.3%; $P = .039$; Fig 2, *F*), similar to the reduced AVF patency in female humans. These findings suggest that reduced AVF patency in female mice may be due to altered hemodynamics during AVF maturation.

Altered hemodynamics in female mice after AVF creation. Because female mice had reduced velocity of blood flow as well as reduced mean magnitude of shear stress in the IVC at baseline (Fig 1, *C*), we used ultrasound to determine whether there were differences in hemodynamics during early AVF remodeling, that is, during postoperative days 1 to 21 (Fig 3, *A*). As expected,[15] mean velocity significantly increased in the IVC after AVF creation, in both female and male mice (Fig 3, *B*). However, on postoperative days 3 and 7, female mice had significantly lower mean velocity in the IVC (Fig 3, *B, upper panel*); female mice also had slightly reduced velocity in the aorta on postoperative day 3 (Fig 3, *B, lower panel*). Similarly, blood flow in both the IVC and the aorta also increased postoperatively, with reduced blood flow in female mice (Fig 3, *C*). In addition, the mean magnitude of laminar shear stress in the IVC and the aorta increased after AVF creation in both female and male mice (Fig 3, *D*), with reduced mean laminar shear stress magnitude in female mice in the IVC (Fig 3, *D, upper panel*) but not in the aorta (Fig 3, *D, lower panel*). These findings suggest that female mice have reduced laminar shear stress in the IVC during early AVF remodeling (day 21) compared with male mice.

Because increased magnitudes of shear stress after AVF creation can result in altered shear stress frequencies, reflected by nonlaminar and disturbed flow patterns,[18] we calculated the amount of spectral broadening in the IVC as a measurement of the nonlaminar characteristics of the blood flow. Spectral broadening was increased in the IVC of female mice during early AVF remodeling, with significant difference on postoperative day 7 (Fig 3, *E*). These findings suggest that reduced laminar shear stress in the IVC of female mice during early AVF remodeling (day 21) precedes reduced AVF patency (day 42) in female mice.

Female mice express less Krüppel-like factor 2 (KLF2), endothelial nitric oxide synthase (eNOS), and vascular cell adhesion molecule 1 (VCAM-1) in the AVF. Both KLF2 and eNOS are anti-inflammatory and anti-proliferative in endothelial cells and have increased activity with laminar shear stress.[19-22] In addition, VCAM-1 is responsive to changes in shear stress.[23] The number of baseline messenger RNA (mRNA) transcripts of KLF2, eNOS, and VCAM-1 in the venous wall was similar in female and male mice; however, these mRNA transcripts increased after early AVF remodeling in male mice but not in female mice (Fig 4, *A*). Similarly, protein expression of KLF2, eNOS, and VCAM-1 was similar at

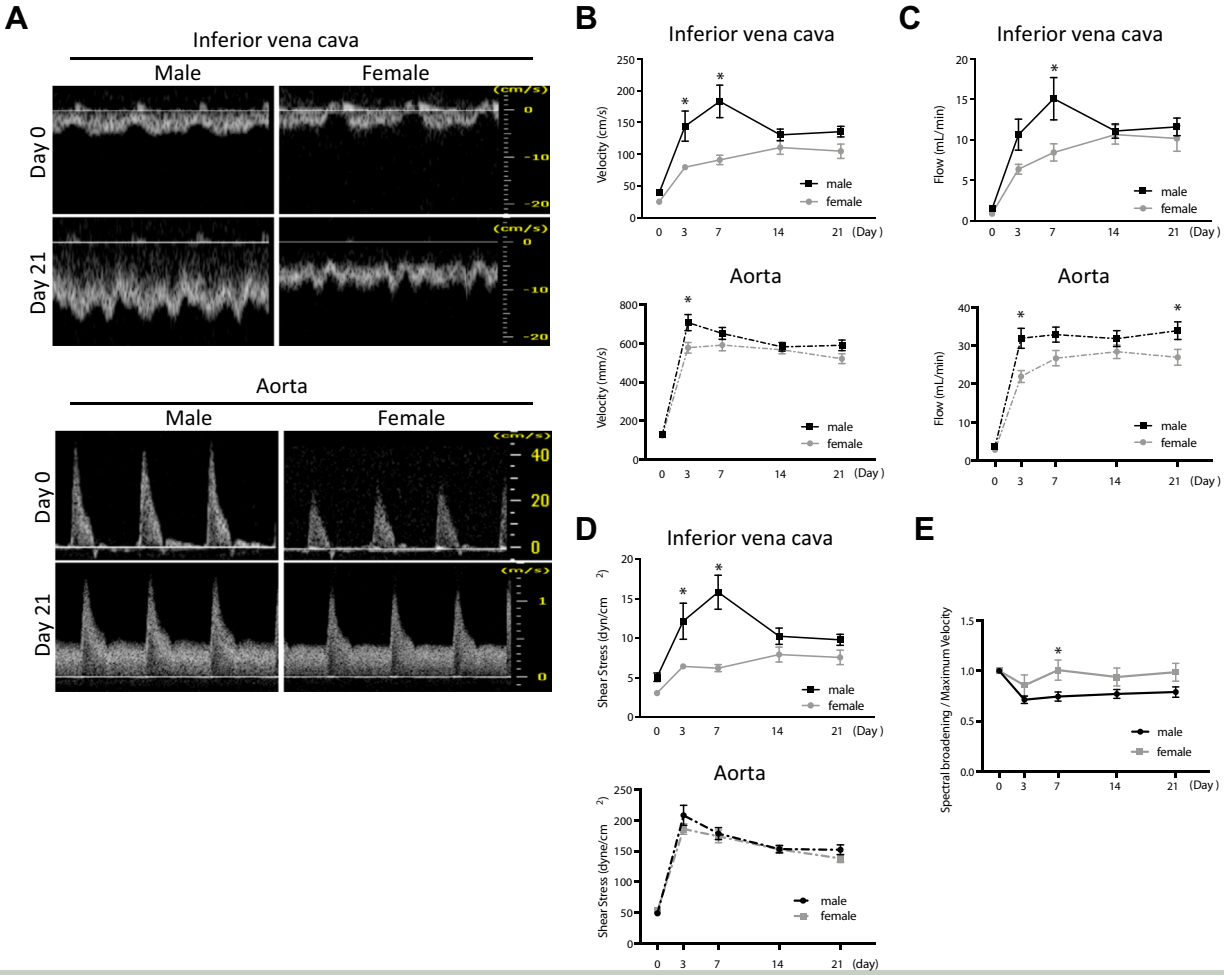

Fig 3. Altered hemodynamics in female mice during early arteriovenous fistula (AVF) remodeling. **A,** Representative preoperative (day 0) and postoperative (day 21) waveforms in inferior vena cava (IVC; *top panel*) and aorta (*bottom panel*) of male vs female mice observed with Doppler ultrasound. **B,** *Top panel*, Line graph showing IVC velocity ($P < .0001$, analysis of variance [ANOVA]; *$P = .0024$ [post hoc] at day 3 and *$P < .0001$ [post hoc] at day 7). *Bottom panel*, Line graph showing aorta velocity ($P < .0001$, ANOVA; *$P = .0056$ at day 3; n = 19-21). **C,** *Top panel*, Line graph showing flow in IVC ($P < .0001$, ANOVA; *$P = .0028$ [post hoc] at day 7). *Bottom panel*, Line graph showing flow in aorta ($P < .0001$, ANOVA; *$P = .0009$ [post hoc] at day 3 and *$P = .0402$ [post hoc] at day 21; n = 19-21). **D,** *Top panel*, Line graph showing shear stress in IVC ($P < .0001$, ANOVA; *$P = .0029$ [post hoc] at day 3 and *$P < .0001$ [post hoc] at day 7) in male vs female mice. *Bottom panel*, Line graph showing shear stress in aorta ($P = .3167$, ANOVA) of male vs female mice (n = 19-21). **E,** Line graph showing spectral broadening to maximum velocity ratio in IVC of male vs female mice ($P = .0376$, ANOVA; day 7, *$P = .0371$; n = 14-15).

baseline in female and male mice but increased in the AVF only in male mice but not in female mice (Fig 4, *B* and *C*). These findings suggest that early AVF remodeling in female mice is associated with lack of increased transcription and translation of several proteins associated with inflammatory, proliferative, and laminar flow responses.

Sex-specific translational differences during AVF maturation. The lower amounts of KLF2, eNOS, and VCAM-1 mRNA and protein in female mice suggest that there may be global differences in protein expression during early AVF remodeling between female mice and male mice. To identify these differences, we performed a proteomic-based comparison of the venous limb of the AVF between female mice and male mice at postoperative day 7. A total of 111,408 different spectra were identified, corresponding to 2171 distinct proteins in both female mice and male mice (Fig 5, *A*). Among these 2171 proteins, only 56 proteins were expressed at significantly higher levels in the IVC of female mice (Table I), and 67 proteins were expressed at significantly higher levels in the IVC of male mice (Table II). Pathway and function-specific analysis of these proteins suggested that the IVC of male mice overexpressed proteins that belong to pathways implicated in the regulation of vascular function (Fig 5, *B*), thrombosis (Fig 5, *C*), response to flow (Fig 5, *D*), and vascular remodeling, including

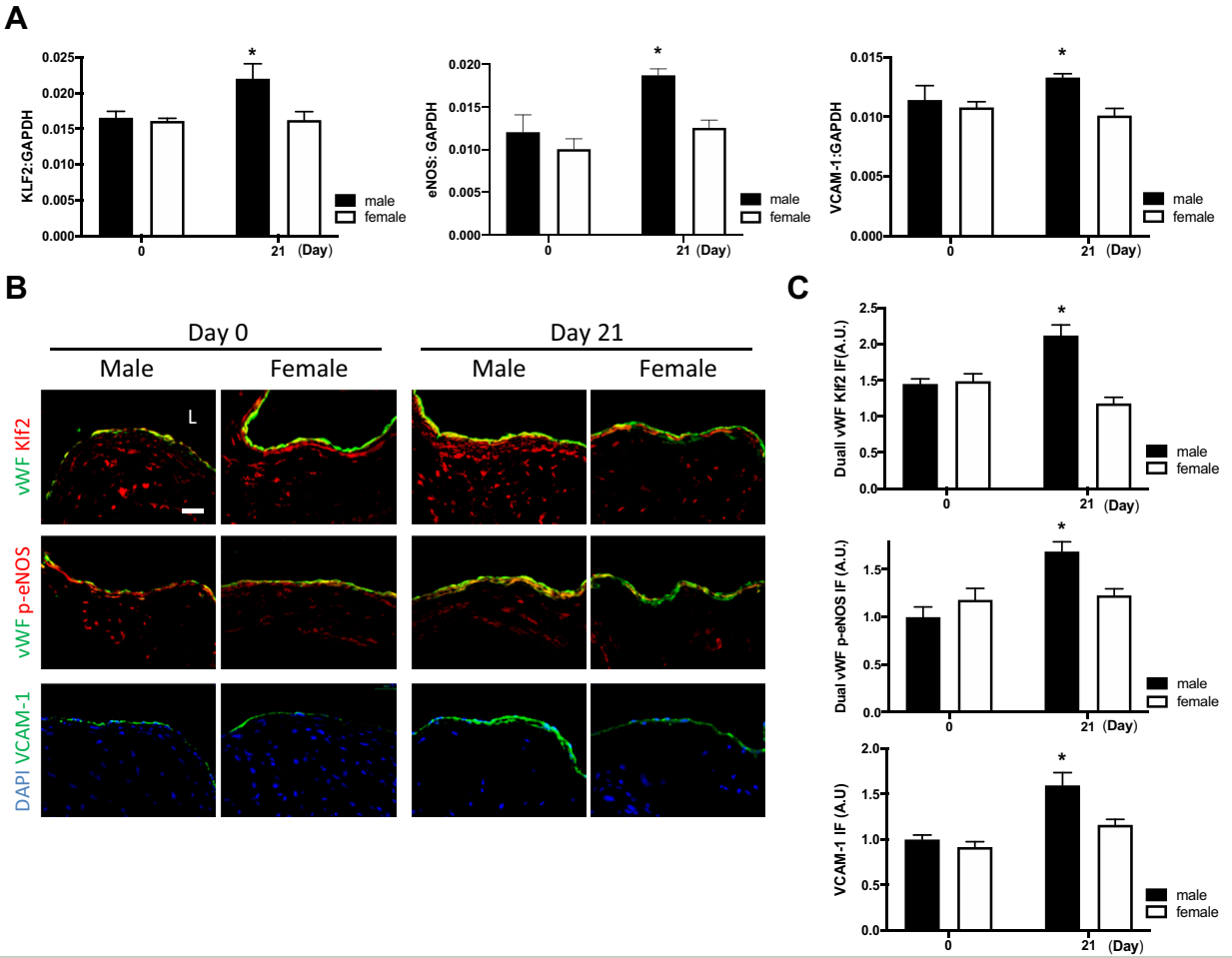

Fig 4. Female mice express less Krüppel-like factor 2 (*KLF2*), endothelial nitric oxide synthase (*eNOS*), and vascular cell adhesion molecule 1 (*VCAM-1*) during early arteriovenous fistula (AVF) remodeling. **A,** Bar graphs show messenger RNA (mRNA) expression of KLF2 in the venous limb of the AVF ($P = .0195$, analysis of variance [ANOVA]; $^*P = .0108$ [post hoc] day 3 vs day 21), *p*-eNOS ($P = .0145$, ANOVA; $^*P = .00{,}318$ [post hoc] at day 21; n = 4-5), and VCAM-1 ($P < .0001$, ANOVA; $^*P < .0001$ [post hoc] day 3 vs day 21; n = 4). **B,** Photomicrographs representative of dual immunofluorescence (*IF*) of von Willebrand factor (*vWF, green*) and KLF2 (*red, first row*) or *p*-eNOS (*red, second row*) or 4′,6-diamidino-2-phenylindole (*DAPI, blue*) and VCAM-1 (*green, third row*) in male vs female AVF, day 3 vs day 21. *L,* Lumen; *scale bar,* 25 μm. **C,** Bar graphs showing quantification of IF in AVF of male vs female mice; vWF KLF2: $P = .0010$, ANOVA (day 3 vs day 21, $^*P < .0001$); vWF *p*-eNOS: $P = .0022$, ANOVA (day 3 vs day 21, $^*P = .0425$, post-hoc); VCAM-1: $P < .0001$, ANOVA (day 3 vs day 21, $^*P = .0007$, post hoc; n = 4-5). *GAPDH,* Glyceraldehyde-3-phosphate dehydrogenase.

extracellular matrix-related proteins (integrin α_{IIb}, integrin β_1, integrin β_3, integrin-linked protein kinase, collagen α1(I) chain, fibulin 2, multimerin 2, and tubulin β1 chain) as well as the tyrosine protein kinases Lyn and Src that regulate the response to laminar flow (Fig 5, *D*). These data suggest that differences in AVF patency between female mice and male mice correspond to different patterns of expression of pathways that regulate the response to laminar flow as well as thrombosis and venous remodeling.

DISCUSSION

This study shows that female C57BL/6 mice have similar dilation and wall thickening during early AVF remodeling (day 21) but reduced patency (day 42) compared with male mice (Fig 2). At baseline, female mice have reduced mean velocity as well as mean magnitude of shear stress in the IVC (Fig 1). After AVF creation, female mice continue to have reduced laminar shear stress in the IVC during early AVF remodeling compared with male mice (Fig 3). Moreover, AVF maturation in female mice is associated with lack of increased expression of several proteins implicated in regulation of inflammation, proliferation, laminar flow responses, thrombosis, and venous remodeling (Figs 4 and 5). These findings suggest that there is a sex difference in patency of the mouse aortocaval fistula, and laminar shear stress magnitude as well as expression of laminar flow response proteins may play a role in the diminished AVF patency in female mice.

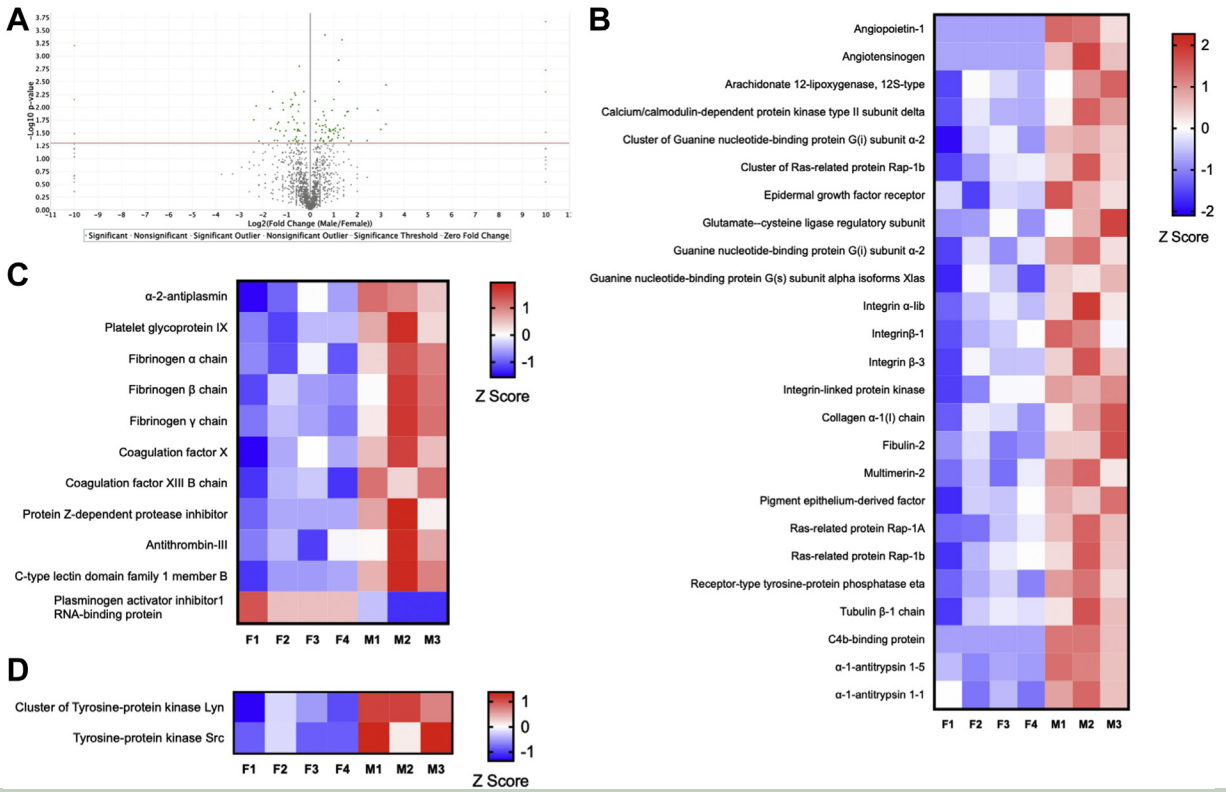

Fig 5. Sex-specific translational differences during early arteriovenous fistula (AVF) remodeling. **A,** Volcano plot showing 111,408 different spectra corresponding to 2171 distinct proteins that were identified in AVF harvested on postoperative day 7. **B-D,** The heatmaps show significantly differentially expressed proteins between female (*F*) and male (*M*) AVF (two-tailed Student *t*-test, false discovery rate <1%; S0 = 2; n = 3-4). The rows represent each of the four samples of female (*left*) and three samples of male (*right*) AVF from individual mice. The *Z* score represents the difference in regulation, with *red* indicating upregulation and *blue* indicating downregulation. Heatmaps are organized by proteins implicated in **(B)** vascular function, **(C)** thrombosis, and **(D)** response to oscillatory or laminar flow.

Our primary finding is that female mice have reduced AVF patency compared with male mice by postoperative day 42 (Fig 2, *F*); we believe that reduced AVF patency in female mice is due to the hemodynamic differences present in female mice and male mice during early AVF remodeling rather than early structural changes, such as vessel dilation and wall thickening. At baseline, female mice have reduced venous shear stress but similar diameter compared with male mice (Fig 1); during AVF maturation, female mice maintain reduced shear stress (Fig 3, *D*) at early times despite similar diameter expansion (Fig 2, *B*). These findings differ from those of several studies suggesting that human women have reduced AVF maturation. For example, Robbin et al[24] reported that women were less likely to reach the minimum fistula diameter of 0.4 cm that was adequate for successful needle placement. Other studies showed that women tend to have prolonged time to AVF maturation compared with men.[7,25] In this study, we did not observe differences in vessel dilation or wall thickening between female mice and male mice (Fig 2); however, we did not perform histologic analysis on failed fistulas, so we cannot attribute AVF failure to excessive neointimal hyperplasia.

Altered hemodynamic forces such as increased shear stress are thought to be necessary for human AVF maturation; shear stress is characterized by both magnitude and frequency (direction). In the cephalic limb of the human brachial-cephalic fistula, shear stress magnitude increases from 5 to 10 dyn/cm^2 preoperatively to 24.5 dyn/cm^2 after 1 week and then normalizes to 10.4 dyn/cm^2 during 3 months.[26,27] Lower magnitudes of shear stress have been associated with higher levels of neointimal hyperplasia as measured in a canine AVF model.[28] In our study, we observed an initial steep increase in shear stress magnitude that then plateaus (Fig 3), similar to that observed in human studies. Interestingly, the change in shear stress after AVF creation is accompanied by increased transcription and translation of proteins associated with inflammatory and laminar flow responses (eNOS, KLF2, and VCAM-1) in male mice but not in female mice. Whether the lack of response in female mice is due to different female-specific biology or purely hemodynamics, such as lower magnitude of shear

Table I. Significantly and differentially expressed proteins in arteriovenous fistula (AVF) of female mice (*t*-test, adjusted $P < .01$)

Identified proteins	Protein description	Fold change
Aars	Alanine-tRNA ligase, cytoplasmic	1.6
Abracl	Costars family protein ABRACL	2.2
Acad10	Acyl-CoA dehydrogenase family member 10	5.2
Aldh4a1	Delta-1-pyrroline-5-carboxylate dehydrogenase, mitochondrial	1.9
Arl3	ADP-ribosylation factor-like protein 3	4.5
Basp1	Brain acid soluble protein 1	1.7
Ces1c	Carboxylesterase 1C	1.4
Chchd6	MICOS complex subunit Mic25	2.2
Cops4	COP9 signalosome complex subunit 4	2.6
Cp	Ceruloplasmin	1.8
Crip2	Cysteine-rich protein 2	1.4
Cyb5a	Cytochrome b_5	1.2
Cyc1	Cytochrome c_1, heme protein, mitochondrial	1.7
Ddah1	N(G),N(G)-dimethylarginine dimethylaminohydrolase 1	1.7
Fkbp1a	Peptidyl-prolyl cis-trans isomerase FKBP1A	1.6
G3bp1	Ras GTPase-activating protein-binding protein 1	1.4
H2afx	Histone H2AX	1.3
Hibadh	3-Hydroxyisobutyrate dehydrogenase, mitochondrial	2.2
Hist1h2af	Cluster of histone H2A type 1-F	1.4
Hist1h2af	Histone H2A type 1-F	1.4
Hist1h4a	Histone H4	1.2
Hist2h2aa1	Histone H2A type 2-A	1.5
Hist2h2ab	Histone H2A type 2-B	1.2
Hnrnpa0	Heterogeneous nuclear ribonucleoprotein A0	1.4
Lmnb2	Lamin-B2	1.5
Lonp1	Lon protease homologue, mitochondrial	2.5
Metap2	Methionine aminopeptidase 2	3.2
Nudc	Nuclear migration protein nudC	4.9
Nudt21	Cleavage and polyadenylation specificity factor subunit 5	2.6
Pbdc1	Protein PBDC1 OS=Mus musculus	5.2
Pcca	Propionyl-CoA carboxylase alpha chain, mitochondrial	2.9
Pcyox1	Prenylcysteine oxidase	2.6
Pdhb	Pyruvate dehydrogenase E1 component subunit beta, mitochondrial	2.2
Psma7	Proteasome subunit alpha type 7	1.4
Psmc5	26S proteasome regulatory subunit 8	1.4
Rmdn1	Regulator of microtubule dynamics protein 1	5.2
Rpl17	60S ribosomal protein L17	1.5
Rpl18a	60S ribosomal protein L18a	3
Rpl36a	60S ribosomal protein L36a	1.7
Rplp2	60S acidic ribosomal protein P2	1.4
Rps23	40S ribosomal protein S23	3.2
Rps26	40S ribosomal protein S26	1.8
Rps27a	Cluster of ubiquitin-40S ribosomal protein S27a	1.2
Rps27a	Ubiquitin-40S ribosomal protein S27a	1.2
S100a4	Protein S100-A4	1.5
Sdhb	Succinate dehydrogenase [ubiquinone] iron-sulfur subunit, mitochondrial	1.5
Serbp1	Plasminogen activator inhibitor 1 RNA-binding protein	1.6
Set	Protein SET	1.7
Sf3b1	Splicing factor 3B subunit 1	1.9
Srsf7	Serine/arginine-rich splicing factor 7	2.8
Stx4	Syntaxin-4	3
Trip10	Cdc42-interacting protein 4	4.5
U2af2	Splicing factor U2AF 65-kDa subunit	2.4
Vapb	Vesicle-associated membrane protein-associated protein B	1.7
Vcp	Transitional endoplasmic reticulum ATPase	1.1

stress, is unclear. Comparing the expression levels of these proteins in female and male endothelial cells in vitro could be helpful. Increasing laminar flow through exercising may be another helpful experiment to better delineate the difference between AVF hemodynamics in female and male mice.

Increased shear stress can also result from increased frequency that reflects altered characteristics of blood flow; flow patterns such as nonlaminar and disordered and even turbulent flow can occur.[18] Using phase-contrast magnetic resonance imaging, Taylor et al[29] showed less diastolic flow reversal in the infrarenal aorta in women compared with men that is a different amount of oscillatory shear stress. Although these data suggest a role for shear stress in the etiology and progression of aortic aneurysms in women and men, these observations further suggest that differences in hemodynamics between women and men may play a general role in the vascular remodeling, including AVF maturation, that likely depends on arterial inflow through the fistula into the venous outflow. Our finding of increased spectral broadening in female IVC (Fig 3)

Table II. Significantly and differentially expressed proteins in arteriovenous fistula (AVF) of male mice (*t*-test, adjusted $P < .01$)

Protein description	Identified proteins	Fold change
Actl6a	Actin-like protein 6A	1.4
Agt	Angiotensinogen	3.5
Alox12	Arachidonate 12-lipoxygenase, 12S-type	1.7
Angpt1	Angiopoietin-1	2.7
Atp1b3	Sodium/potassium-transporting ATPase subunit beta 3	1.7
C4bpa	C4b-binding protein	3.4
Camk2d	Calcium/calmodulin-dependent protein kinase type II subunit delta	5.1
Capn1	Calpain-1 catalytic subunit	3.3
Clca3a1	Calcium-activated chloride channel regulator 3A-1	1.2
Clta	Clathrin light chain A	1.2
Col1a1	Collagen alpha-1(I) chain	1.5
Comtd1	Catechol *O*-methyltransferase domain-containing protein 1	1.5
Copb2	Coatomer subunit beta	1.6
Cpb2	Carboxypeptidase B2	1.7
Ddx39b	Spliceosome RNA helicase Ddx39b	1.9
Dhrs7	Dehydrogenase/reductase SDR family member 7	2.8
Dnajc5	DnaJ homolog subfamily C member 5	1.2
Dpep1	Dipeptidase 1	1.5
Egfr	Epidermal growth factor receptor	1.2
F10	Coagulation factor X	1.4
F13b	Coagulation factor XIII B chain	1.5
Fbln2	Fibulin 2	2.5
Fga	Fibrinogen alpha chain	3.3
Fgb	Fibrinogen beta chain	1.2
Fgg	Fibrinogen gamma chain	1.2
Fscn1	Fascin	3.5
Fyb1	FYN-binding protein 1	2.8
Gclm	Glutamate-cysteine ligase regulatory subunit	3
Gnai2	Guanine nucleotide-binding protein G_i subunit alpha-2	1.6
Gp9	Platelet glycoprotein IX	2.4
H2-Q10	H-2 class I histocompatibility antigen, Q10 alpha chain	3.1
Hp	Haptoglobin	2.6
Ifitm3	Interferon-induced transmembrane protein 3	2.1
Ilk	Integrin-linked protein kinase	1.4
Itga2b	Integrin alpha-IIb	1.9
Itgb1	Integrin beta-1	1.7
Itgb3	Integrin beta-3	1.2
Lgmn	Legumain	1.7
Lyn	Cluster of tyrosine-protein kinase Lyn	1.5
Mfap5	Microfibrillar-associated protein 5	1.8
Mmrn2	Multimerin 2	3.4
Mug1	Murinoglobulin 1	5.1
Myl9	Myosin regulatory light polypeptide 9	3.3
Pck2	Phosphoenolpyruvate carboxykinase [GTP], mitochondrial	1.2
Pdlim4	PDZ and LIM domain protein 4	2.8
Pgm5	Phosphoglucomutase-like protein 5	3.8
Plcg2	1-Phosphatidylinositol 4,5-bisphosphate phosphodiesterase gamma-2	2.1

(Continued on next page)

Table II. Continued.

Protein description	Identified proteins	Fold change
Ppif	Peptidyl-prolyl cis-trans isomerase F, mitochondrial	2.7
Ptprj	Receptor-type tyrosine-protein phosphatase eta	1.8
Rab14	Ras-related protein Rab-14	1.4
Rap1a	Ras-related protein Rap-1A	2.9
Rap2b	Ras-related protein Rap-2b	3.4
Rasa3	Ras GTPase-activating protein 3	4.2
Rasgrp2	RAS guanyl-releasing protein 2	1.7
Rpsa	40S ribosomal protein SA	2.8
Serpina10	Protein Z-dependent protease inhibitor	3.1
Serpina1a	Alpha-1-antitrypsin 1-1	3
Serpina1e	Alpha-1-antitrypsin 1-5	1.6
Serpinc1	Antithrombin-III	1.4
Serpine2	Glia-derived nexin	1.3
Serpinf1	Pigment epithelium-derived factor	2.2
Serpinf2	Alpha-2-antiplasmin	1.4
Slc2a3	Solute carrier family 2, facilitated glucose transporter member 3	1.4
Src	Neuronal proto-oncogene tyrosine-protein kinase Src	2.1
Sytl4	Synaptotagmin-like protein 4	2.3
Treml1	Trem-like transcript 1 protein	1.8
Tubb1	Tubulin beta-1 chain	1.4

suggests less laminar flow as an upstream regulator of different molecular pathways, including less activation of atheroprotective signaling (Figs 4 and 5).[19] Although the absolute magnitude of spectral broadening will increase if the velocity increases, the retained increased relative spectral broadening—defined as the ratio of spectral broadening to maximum velocity—suggests there is less laminar flow in female mice (Fig 3, *E*). Interestingly, an unbiased proteomic comparison between female and male AVF showed sex-specific differences in multiple classes of proteins, including those involved in vascular function (Fig 5, *B*), thrombosis (Fig 5, *C*), and response to laminar flow as well as vascular remodeling (Fig 5, *D*).

The cause of sex-specific differences in our model as well as in human AVF patency and utilization is not clear. Although estrogen plays an atheroprotective role in premenopausal women, little is known about the hormonal status of women on hemodialysis. Dorsett-Martin and Hester[30] used a rat aortocaval AVF model to study the role of sex hormones in aortic wall thickness after AVF; estrogen administration in castrated male rats decreased aortic wall thickness, whereas testosterone administration in ovariectomized female rats increased aortic wall thickness.[30] Our proteomic analysis did not show any significant differences related to estrogen signaling; however, we used young mice in this study, comparable to our previous data. Because most dialysis patients are postmenopausal, the choice of young animals may not reflect differences in older animals. An older oophorectomy model, with comparable age and menopausal status to humans requiring AVF, might be useful to control for this confounding variable. In addition, the size of vessels in mice and humans is different, and thus our data in mice might not be translatable to humans; studies in larger animals might provide more clinically relevant analyses. Furthermore, we did not examine a uremic mouse model that has different expression of several relevant genes.[31] Proteomic data are derived from the whole vessel wall and not limited to endothelial cells. In addition, strain calculations using advanced ultrasound systems may be useful and a surrogate for compliance data. Moreover, it would be of interest to assess additional data, such as the mechanical properties of the vessel wall, perianastomotic thrombus formation, and any potential change in size of the aortocaval fistula opening over time, as these factors may also be contributing to the difference in patency between female mice and male mice.

CONCLUSIONS

This study shows that there is a sex difference in AVF patency in an aortocaval mouse model. AVF in female mice have lower velocity, flow, and magnitudes of shear stress as well as less laminar flow without any differences in dilation or wall thickening. Differences in AVF patency

between female and male mice also correspond with different patterns of expression of pathways that regulate the response to laminar flow as well as thrombosis and venous remodeling. It is important to identify downstream targets involved in these mechanisms to improve AVF outcomes in female patients.

AUTHOR CONTRIBUTIONS

Conception and design: TK, SO, AF, JK, TN, AD
Analysis and interpretation: TK, SO, AF, TI, HH
Data collection: TK, SO, AF, LG, BY, RT
Writing the article: TK, AF
Critical revision of the article: SO, LG, TI, HH, BY, RT, JK, TN, AD
Final approval of the article: TK, SO, AF, LG, TI, HH, BY, RT, JK, TN, AD
Statistical analysis: TK, SO, AF
Obtained funding: AD
Overall responsibility: AD
TK, SO, and AF contributed equally to this article and share co-first authorship.

REFERENCES

1. Dixon BS, Novak L, Fangman J. Hemodialysis vascular access survival: upper-arm native arteriovenous fistula. Am J Kidney Dis 2002;39:92-101.
2. Anel RL, Yevzlin AS, Ivanovich P. Vascular access and patient outcomes in hemodialysis: questions answered in recent literature. Artif Organs 2003;27:237-41.
3. Roy-Chaudhury P, Kelly BS, Melhem M, Zhang J, Li J, Desai P, et al. Vascular access in hemodialysis: issues, management, and emerging concepts. Cardiol Clin 2005;23:249-73.
4. Hu H, Patel S, Hanisch JJ, Santana JM, Hashimoto T, Bai H, et al. Future research directions to improve fistula maturation and reduce access failure. Semin Vasc Surg 2016;29:153-71.
5. Bashar K, Zafar A, Elsheikh S, Healy DA, Clarke-Moloney M, Casserly L, et al. Predictive parameters of arteriovenous fistula functional maturation in a population of patients with end-stage renal disease. PLoS One 2015;10:e0119958.
6. Peterson WJ, Barker J, Allon M. Disparities in fistula maturation persist despite preoperative vascular mapping. Clin J Am Soc Nephrol 2008;3:437-41.
7. Dunn J, Herscu G, Woo K. Factors influencing maturation time of native arteriovenous fistulas. Ann Vasc Surg 2015;29:704-7.
8. Almasri J, Alsawas M, Mainou M, Mustafa RA, Wang Z, Woo K, et al. Outcomes of vascular access for hemodialysis: a systematic review and meta-analysis. J Vasc Surg 2016;64:236-43.
9. Miller CD, Robbin ML, Allon M. Gender differences in outcomes of arteriovenous fistulas in hemodialysis patients. Kidney Int 2003;63:346-52.
10. Farber A, Imrey PB, Huber TS, Kaufman JM, Kraiss LW, Larive B, et al. Multiple preoperative and intraoperative factors predict early fistula thrombosis in the Hemodialysis Fistula Maturation Study. J Vasc Surg 2016;63:163-70.e6.
11. Allon M, Ornt DB, Schwab SJ, Rasmussen C, Delmez JA, Greene T, et al. Factors associated with the prevalence of arteriovenous fistulas in hemodialysis patients in the HEMO study. Hemodialysis (HEMO) Study Group. Kidney Int 2000;58:2178-85.
12. Pisoni RL, Young EW, Dykstra DM, Greenwood RN, Hecking E, Gillespie B, et al. Vascular access use in Europe and the United States: results from the DOPPS. Kidney Int 2002;61:305-16.
13. Allon M, Lockhart ME, Lilly RZ, Gallichio MH, Young CJ, Barker J, et al. Effect of preoperative sonographic mapping on vascular access outcomes in hemodialysis patients. Kidney Int 2001;60:2013-20.
14. Yamamoto K, Li X, Shu C, Miyata T, Dardik A. Technical aspects of the mouse aortocaval fistula. J Vis Exp 2013;77:e50449.
15. Yamamoto K, Protack CD, Tsuneki M, Hall MR, Wong DJ, Lu DY, et al. The mouse aortocaval fistula recapitulates human arteriovenous fistula maturation. Am J Physiol Heart Circ Physiol 2013;305:H1718-25.
16. Nesvizhskii AI, Keller A, Kolker E, Aebersold R. A statistical model for identifying proteins by tandem mass spectrometry. Anal Chem 2003;75:4646-58.
17. Ashburner M, Ball CA, Blake JA, Botstein D, Butler H, Cherry JM, et al. Gene ontology: tool for the unification of biology. The Gene Ontology Consortium. Nat Genet 2000;25:25-9.
18. Krishnamoorthy MK, Banerjee RK, Wang Y, Zhang J, Sinha Roy A, Khoury SF, et al. Hemodynamic wall shear stress profiles influence the magnitude and pattern of stenosis in a pig AV fistula. Kidney Int 2008;74:1410-9.
19. SenBanerjee S, Lin Z, Atkins GB, Greif DM, Rao RM, Kumar A, et al. KLF2 is a novel transcriptional regulator of endothelial proinflammatory activation. J Exp Med 2004;199:1305-15.
20. Guzman RJ, Abe K, Zarins CK. Flow-induced arterial enlargement is inhibited by suppression of nitric oxide synthase activity in vivo. Surgery 1997;122:273-9; discussion: 279-80.
21. Liang A, Wang Y, Han G, Truong L, Cheng J. Chronic kidney disease accelerates endothelial barrier dysfunction in a mouse model of an arteriovenous fistula. Am J Physiol Renal Physiol 2013;304:F1413-20.
22. Croatt AJ, Grande JP, Hernandez MC, Ackerman AW, Katusic ZS, Nath KA. Characterization of a model of an arteriovenous fistula in the rat: the effect of L-NAME. Am J Pathol 2010;176:2530-41.
23. Lorenz M, Koschate J, Kaufmann K, Kreye C, Mertens M, Kuebler WM, et al. Does cellular sex matter? Dimorphic transcriptional differences between female and male endothelial cells. Atherosclerosis 2015;240:61-72.
24. Robbin ML, Chamberlain NE, Lockhart ME, Gallichio MH, Young CJ, Deierhoi MH, et al. Hemodialysis arteriovenous fistula maturity: US evaluation. Radiology 2002;225:59-64.
25. Jemcov TK. Morphologic and functional vessels characteristics assessed by ultrasonography for prediction of radiocephalic fistula maturation. J Vasc Access 2013;14:356-63.
26. Corpataux JM, Haesler E, Silacci P, Ris HB, Hayoz D. Low-pressure environment and remodelling of the forearm vein in Brescia-Cimino haemodialysis access. Nephrol Dial Transplant 2002;17:1057-62.
27. Manning E, Skartsis N, Orta AM, Velazquez OC, Liu ZJ, Asif A, et al. A new arteriovenous fistula model to study the development of neointimal hyperplasia. J Vasc Res 2012;49:123-31.
28. Jia L, Wang L, Wei F, Yu H, Dong H, Wang B, et al. Effects of wall shear stress in venous neointimal hyperplasia of arteriovenous fistulae. Nephrology (Carlton) 2015;20:335-42.

29. Taylor WR, Iffrig E, Veneziani A, Oshinski JN, Smolensky A. Sex and vascular biomechanics: a hypothesis for the mechanism underlying differences in the prevalence of abdominal aortic aneurysms in men and women. Trans Am Clin Climatol Assoc 2016;127:148-61.
30. Dorsett-Martin WA, Hester RL. Sex hormones and aortic wall remodeling in an arteriovenous fistula. Gend Med 2007;4: 157-69.
31. Misra S, Shergill U, Yang B, Janardhanan R, Misra KD. Increased expression of HIF-1α, VEGF-A and its receptors, MMP-2, TIMP-1, and ADAMTS-1 at the venous stenosis of arteriovenous fistula in a mouse model with renal insufficiency. J Vasc Interv Radiol 2010;21:1255-61.

Submitted Dec 16, 2019; accepted Mar 6, 2020.

Supplementary Table I. Primer sequences

VCAM1	Forward	5′-ATGTCAACGTTGCCCCCAA
	Reverse	5′-CAGGACTGCCCTCCTCTAGT
eNOS	Forward	5′-ACGCACCCAGAGCTTTTCTT
	Reverse	5′-TGCAACCAATGCTGTAGGCA
KFL2	Forward	5′-TGCACGCGTGGGGGCCCGAGT
	Reverse	5′-CGGGGAAAGCGCGGGCACT
GAPDH	Forward	5′-AATGTGTCCGTCGTGGATCTGA
	Reverse	5′-AGTGTAGCCCAAGATGCCCTTC

Supplementary Table II. List of antibodies

Target antigen	Vendor or source	Catalog No.
VCAM1	Abcam	ab134047
phospho-eNOS	Abcam	ab195944
KLF2	LifeSpan BioSciences	LS-C502181
vWF	Abcam	ab11713

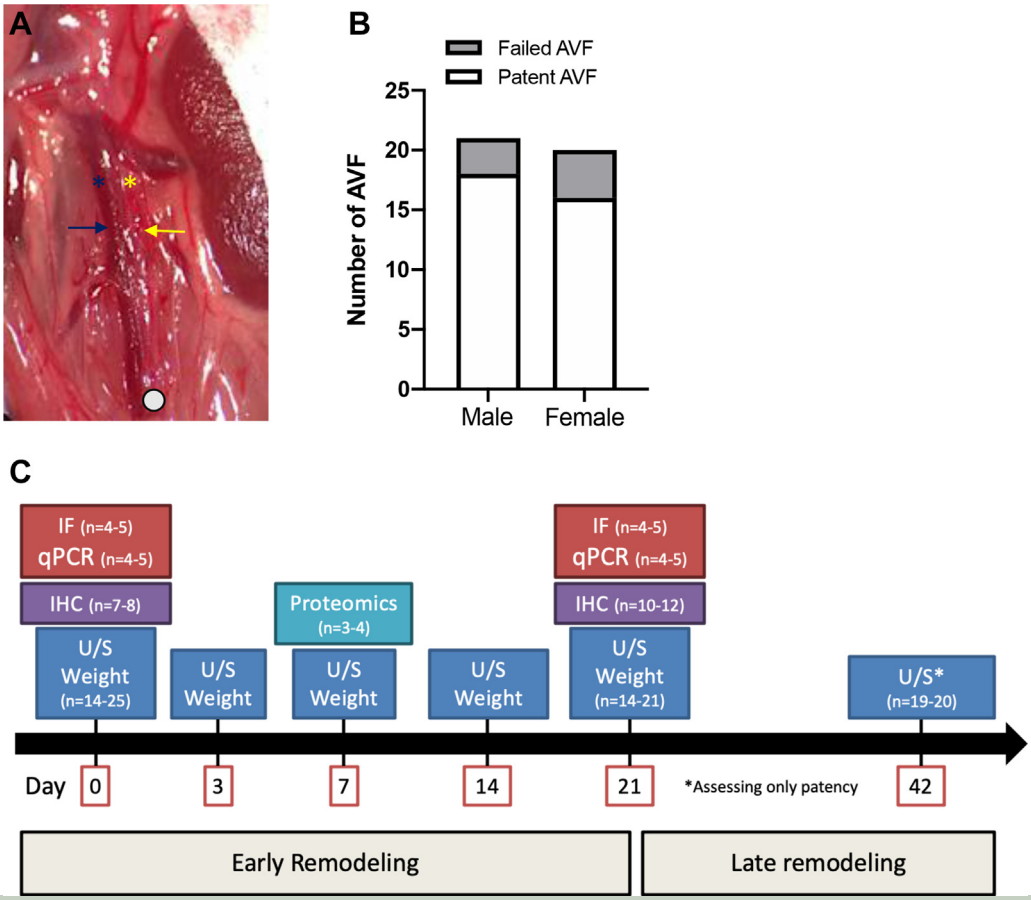

Supplementary Fig. A, Operative photograph with transperitoneal tissue dissected to expose the aorta and the inferior vena cava (IVC) in a mouse aortocaval fistula; *blue and yellow arrows* denote the IVC and the aorta, respectively; *blue and yellow asterisks* denote where the ultrasound probe was placed for measurements in the infrarenal IVC and the aorta, respectively; the *white circle* denotes the site of aortocaval fistula creation. **B,** Bar graph showing the technical success rate of arteriovenous fistula (*AVF*) creation in male (87.8%) compared with female mice (82.5%; $P = .8132$, χ^2). **C,** Flow chart demonstrating the experimental design of this study. *IF,* Immunofluorescence; *IHC,* immunohistochemistry; *qPCR,* quantitative polymerase chain reaction; *U/S,* ultrasound.